research articles Journal of proteome research

Proteomic Identification of Altered Proteins in Skeletal Muscle During Chronic Potassium Depletion: Implications for Hypokalemic Myopathy

Visith Thongboonkerd,*,† Rattiyaporn Kanlaya,†,‡ Supachok Sinchaikul,§ Paisal Parichatikanond,|| Shui-Tein Chen,§,⊥ and Prida Malasit†,#

Medical Molecular Biology Unit, Office for Research and Development, Faculty of Medicine Siriraj Hospital, Mahidol University, Bangkok, Thailand, Department of Immunology, Faculty of Medicine Siriraj Hospital, Mahidol University, Bangkok, Thailand, Institute of Biological Chemistry and Genomic Research Center, Academia Sinica, Taipei, Taiwan, Department of Pathology, Faculty of Medicine Siriraj Hospital, Mahidol University, Bangkok, Thailand, Institute of Biochemical Sciences, College of Life Science, National Taiwan University, Taipei, Taiwan, and Medical Biotechnology Unit, National Center for Genetic Engineering and Biotechnology, National Science and Technology Development Agency, Bangkok, Thailand

Received April 2, 2006

Prolonged potassium depletion is a well-known cause of myopathy. The pathophysiology of hypokalemic myopathy, however, remains unclear. We performed a gel-based, differential proteomics study to define altered proteins in skeletal muscles during chronic potassium depletion. BALB/c mice were fed with normal chow (0.36% K^+) or K^+-depleted (KD) diet (<0.001% K^+) for 8 weeks ($n = 5$ in each group). Left gastrocnemius muscles were surgically removed from each animal. Histopathological examination showed mild-degree infiltration of polymornuclear and mononuclear cells at the interstitium of the KD muscles. Extracted proteins were resolved with two-dimensional electrophoresis (2-DE), and visualized with Coomassie Brilliant Blue R-250 stain. Quantitative intensity analysis revealed 16 up-regulated protein spots in the KD muscles, as compared to the controls. These differentially expressed proteins were subsequently identified by peptide mass fingerprinting and by quadrupole time-of-flight tandem mass spectrometry (Q-TOF MS/MS). Most of the altered proteins induced by chronic potassium depletion were muscle enzymes that play significant roles in several various metabolic pathways. Other up-regulated proteins included myosin-binding protein H, alpha-B Crystallin, and translationally controlled tumor protein (TCTP). These findings may lead to a new roadmap for research on hypokalemic myopathy, to better understanding of the pathophysiology of this medical disease, and to biomarker discovery.

Keywords: potassium • hypokalemia • myopathy • muscle • enzymes • proteomics • proteome

Introduction

Hypokalemia, which is generally defined as a serum K^+ of less than 3.5 mmol/L, is one of the most common electrolyte disorders encountered in clinical practice and found in more than 20% of hospitalized patients.[1] It is also common in outpatients who take thiazide diuretics for treatment of hypertension, with an incidence of up to 48%.[2] Hypokalemia may be asymptomatic if the deficit is temporary and the degree of the deficit is modest to mild (3.0−3.5 mmol/L), but it can be a cause of death when the degree of the deficit is severe (<3.0 mmol/L) and the dysregulation is left untreated. Prolonged K^+ deficiency can affect several organ systems, particularly cardiovascular, gastrointestinal, renal, and musculoskeletal systems.[3−5] Muscular defects from chronic K^+ depletion have been defined as "*hypokalemic myopathy*", a disease known for quite some time, but the molecular mechanisms or the links between K^+ deficiency and muscle injury remain unclear.[6−10]

Previously, several studies had evaluated physiological changes in skeletal muscles during K^+ depletion. These reports, however, focused only on roles of sodium pumps and the balance of cellular cations.[11−13] None of these studies had explored the global alterations in muscle proteins during prolonged K^+ depletion, the information of which may imply the pathogenic mechanisms of hypokalemic myopathy. In the postgenomic era, proteomic technologies are widely available and have been

* To whom correspondence should be addressed. Visith Thongboonkerd, MD, FRCPT, Medical Molecular Biology Unit, Office for Research and Development, 12th Floor Adulyadej Vikrom Building, 2 Prannok Road, Siriraj Hospital, Bangkoknoi, Bangkok 10700, Thailand; Phone/Fax: +66-2-4184793; E-mail: thongboonkerd@dr.com (or) vthongbo@yahoo.com.

† Office for Research and Development, Faculty of Medicine Siriraj Hospital.

‡ Department of Immunology, Faculty of Medicine Siriraj Hospital.

§ Institute of Biological Chemistry and Genomic Research Center.

|| Department of Pathology, Faculty of Medicine Siriraj Hospital.

⊥ National Taiwan University.

National Science and Technology Development Agency.

10.1021/pr060136h CCC: $33.50
Published on Web 11/08/2006

proven to be useful to unravel the pathophysiology of human diseases.[14−16] There are several studies that have applied proteomics to examining skeletal muscle proteome.[17−20] However, none of these available references has adopted proteomics to hypokalemic myopathy.

The present study has utilized proteomic methodology to identify changes in protein expression in skeletal muscles of mice exposed to prolonged K^+ depletion. Hypokalemia was induced by giving *ad libertum* K^+-depleted (KD) diet to BALB/c mice for 8 weeks, whereas the control mice received normal-K^+ chow. A gel-based, differential proteomics study of left gastrocnemius muscles revealed alterations in the expression of 16 muscle proteins in the KD mice. Among these altered proteins, 15 were identified by quadrupole time-of-flight (Q-TOF) mass spectrometry (MS) and tandem mass spectrometry (MS/MS). Functional significance and potential roles of these identified proteins in hypokalemic myopathy are discussed.

Materials and Methods

Animals and Diets. Young male BALB/c mice ($n = 5$ in each group; total $n = 10$) with comparable initial body weights (35.06 ± 1.12 vs 35.82 ± 0.68 g; $p = 0.823$) were used in the present study. They were fed with *ad libertum* normal-K^+ (0.36% K^+; #TD97214; Harland Teklad, Madison, WI) or KD (<0.001% K^+; #TD88239) chow for 8 weeks. All other elements in the diet (including protein, casein, D,L-methionine, sucrose, corn starch, corn oil, cellulose, mixed vitamin, ethoxyquin, calcium phosphate, calcium carbonate, sodium chloride, magnesium oxide, magnesium sulfate, ferric citrate, manganous carbonate, zinc carbonate, cupric carbonate, sodium iodate, and sodium selenite) were identical between the two types of diets. After 8 weeks of differential diets, the mice were sacrificed and the left gastrocnemius muscles were surgically removed for further proteomic analysis. All studies of animals were in accordance with the Institutional Animal Care and Use Committee and The Guide for the Care and Use of Laboratory Animals.

Protein Extraction for Proteomic Analysis. Muscle was excised into several thin slices and the contaminated blood was washed with ice-cold PBS. The tissue was then briskly frozen in liquid nitrogen, ground to powder, resuspended in a buffer containing 7 M urea, 2 M thiourea, 4% 3-[(3-cholamidopropyl)-dimethylamino]-1-propanesulfonate (CHAPS), 2% (v/v) ampholytes (pH 3−10), 120 mM dithiothreitol (DTT), and 40 mM Tris-base, and incubated at 4 °C for 30 min. After low-speed centrifugation (12 000 *g* for 5 min), the supernatant was saved and the protein concentration was measured by spectrophotometry using Bio-Rad Protein Assay (Bio-Rad Laboratories, Hercules, CA) based on Bradford's method. Because urea, thiourea, CHAPS, and other compositions in the sample/lysis buffer can interfere with the protein estimation, we generated the standard curve using bovine serum albumin at the concentrations of 0, 2, 5, 7, and 10 μg/μL in the same sample/lysis buffer to make sure that the standards and the samples had the same background that might occur due to chemical interference. Muscle proteins extracted from each animal were further resolved in individual 2-D gels; $n = 5$ gels (from 5 animals) for each group; total $n = 10$ gels.

Two-Dimensional Electrophoresis (2-DE) and Staining. Immobiline DryStrip, linear pH 3−10, 7-cm long (Amersham Biosciences, Uppsala, Sweden), was rehydrated overnight with 200 μg total protein (equal loading for each sample) that was premixed with rehydration buffer containing 7 M urea, 2 M thiourea, 2% CHAPS, 2% (v/v) ampholytes (pH 3−10), 120 mM DTT, 40 mM Tris-base, and bromophenol blue (to make the final volume of 150 μL per strip). The first dimensional separation (IEF) was performed in Ettan IPGphor II IEF System (Amersham Biosciences) at 20 °C, using stepwise mode to reach 9 000 V·h. After completion of the IEF, proteins on the strip were equilibrated in a buffer containing 6 M urea, 130 mM DTT, 30% glycerol, 112 mM Tris base, 4% sodium dodecyl sulfate (SDS), and 0.002% bromophenol blue for 10 min, and then with another buffer containing 6 M urea, 135 mM iodoacetamide, 30% glycerol, 112 mM Tris base, 4% SDS, and 0.002% bromophenol blue for 10 min. The IPG strip was then transferred onto 12% acrylamide slab gel (8 × 9.5 cm), and the second dimensional separation was performed in SE260 Mini-Vertical Electrophoresis Unit (Amersham Biosciences) with the current 20 μA/gel for 1.5 h. Separated protein spots were then visualized using Coomassie Brilliant Blue R-250 stain (Fluka Chemica AG, Buchs, Switzerland).

Spot Analysis and Matching. Image Master 2D Platinum (Amersham Biosciences) software was used for matching and analysis of protein spots on 2-D gels. Parameters used for spot detection were (i) minimal area = 10 pixels, (ii) smooth factor = 2.0, and (iii) saliency = 2.0. A reference gel was created from an artificial gel combining all of the spots presenting in different gels into one image. The reference gel was then used for matching of corresponding protein spots between gels. Background subtraction was performed and the intensity volume of individual spot was normalized with total intensity volume (summation of the intensity volumes obtained from all spots in the same 2-D gel). Variability of 2-D spot pattern was evaluated by determining the coefficient of variation (CV) of the normalized intensity of corresponding spot across different gels (%CV = standard deviation/mean × 100%). Comparisons between groups were performed using unpaired *t* test. *P* values less than 0.05 were considered statistically significant.

In-Gel Tryptic Protein Digestion. Differentially expressed protein spots were excised from the 2-D gels and the gel pieces were washed with 200 μL of 50% acetonitrile (ACN)/25 mM NH_4HCO_3 buffer (pH 8.0) for 15 min twice. The gel pieces were then washed once with 200 μL of 100% ACN and dried using a Speed Vac concentrator (Savant, Holbrook, NY). Dried gel pieces were swollen with 10 μL of 1% (w/v) trypsin (Promega, Madison WI) in 25 mM NH_4HCO_3. The gel pieces were then crushed with siliconized blue stick and incubated at 37 °C for at least 16 h. Peptides were subsequently extracted twice with 50 μL of 50% ACN/5% trifluoroacetic acid (TFA); the extracted solutions were then combined and dried with the Speed Vac concentrator. The peptide pellets were then resuspended in 10 μL of 0.1% TFA and the resuspended solutions were purified using $ZipTip_{C18}$ (Millipore, Bedford, MA). Ten microliters of sample was drawn up and down in the ZipTip for 10 times and then washed with 10 μL of 0.1% formic acid by drawing up and expelling the washing solution for 3 times. The peptides were finally eluted with 5 μL of 75% ACN/0.1% formic acid.

Protein Identification by Q-TOF MS and MS/MS. The proteolytic samples were premixed 1:1 with the matrix solution (5 mg/mL α-cyano-4-hydroxycinnamic acid (CHCA) in 50% ACN, 0.1% v/v TFA and 2% w/v ammonium citrate) and spotted onto the 96-well MALDI (matrix-assisted laser desorption/ionization) sample stage. The samples were analyzed by the Q-TOF Ultima MALDI instrument (Micromass, Manchester, UK), which was fully automated with predefined probe motion pattern and the peak intensity threshold for switching over from MS survey scanning to MS/MS, and from one MS/MS to

another. Within each sample well, parent ions that met the predefined criteria (any peak within the m/z 800−3000 range with intensity above 10 count ± include/exclude list) were selected for CID MS/MS using argon as the collision gas and a mass dependent ±5 V rolling collision energy until the end of the probe pattern was reached (all details are available at http://proteome.sinica.edu.tw).

For peptide mass fingerprinting, both MASCOT (http://www.matrixscience.com) and ProFound (http://129.85.19.192/profound_bin/WebProFound.exe) search engines were used. Proteins were identified based on the assumptions that peptides were monoisotopic, oxidized at methionine residues and carbamidomethylated at cysteine residues. The search was performed using the mammalian protein database of the NCBI (National Center for Biotechnology Information). A mass tolerance of 50 ppm was used and up to 1 missed trypsin cleavage was allowed. Identities with probability-based MOWSE (molecular weight search) scores > 69 (for MASCOT) and/or Z scores > 1.65 (for ProFound) were considered as "significant hits". For MS/MS peptide sequence identification, the MASCOT search engine was employed. Search parameters allowed were similar to those for PMF. Peptides with ions scores >37 were considered as "significant hits". Only significant hits from peptide mass fingerprinting and/or MS/MS peptide ion search were reported in the Results.

2-D Western Blotting. After the completion of 2-DE as described above, proteins were transferred onto a nitrocellulose membrane and nonspecific bindings were blocked with 5% milk in PBS for 1 h. The membrane was then incubated with rabbit polyclonal anti-β-enolase antibody (1:200 in 5% milk in PBS) (Santa Cruz Biotechnology, Inc., Santa Cruz, CA) at room temperature for 1 h. After washing, the membrane was further incubated with swine anti-rabbit IgG conjugated with horseradish peroxidase (1:1000 in 5% milk in PBS) (Dako, Glostrup, Denmark) at room temperature for 1 h. Reactive protein spots were then visualized with SuperSignal West Pico chemiluminescence substrate (Pierce Biotechnology, Inc., Rockford, IL).

Measurement of Serum Creatine Kinase Levels. Total CK level was measured using a standard Oliver-Rosalki assay, as described previously.[21,22] CK−MM was examined by Western blot analysis. Details of the blotting procedures were the same as described above, except only for the antibody, which was goat anti-CK−MM conjugated with horseradish peroxidase (Biocheck, Inc., Foster City, CA). CK−MB level was measured using a CK−MB Enzyme Immunoassay Kit (Biocheck, Inc.). Positive control was the CK−MB standards containing 0, 7.5, 15, 50, 100, and 200 ng/mL CK−MB. Color intensity was measured spectrophotometrically at λ450 nm.

Results and Discussion

Clinical Data and Histopathological Findings. The mice in both groups had comparable amounts of dietary intake (Figure 1). After 8 weeks of differential diets, the mice were sacrificed and the left gastrocnemius muscles were surgically removed for histopathological examination and proteomic analysis. Plasma K^+ levels on sacrificed date were 4.46 ± 0.23 and 1.51 ± 0.21 mmol/L for control and KD mice, respectively (p < 0.0001). In addition to severe hypokalemia, the KD mice also developed metabolic alkalosis. Plasma HCO_3^- levels were 25.67 ± 0.38 and 31.90 ± 2.11 mmol/L for control and KD mice, respectively (p < 0.005). Histopathological examination using Hematoxylin-Eosin stain showed only mild-degree infiltration of polymorphonuclear and mononuclear cells at some areas

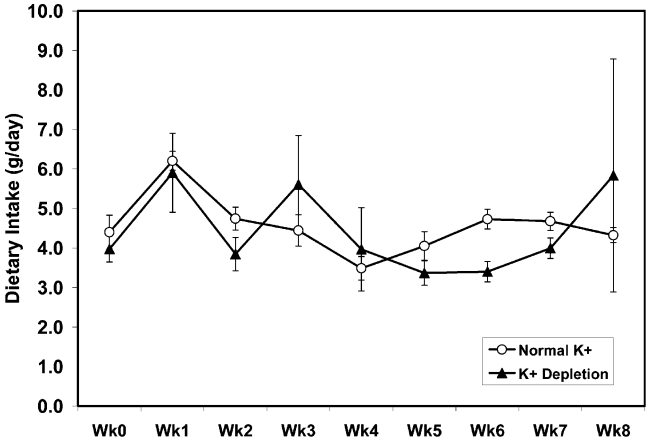

Figure 1. Dietary intake. The animals in both groups had comparable amounts of food intake throughout the study (except at week 2 and 6, when the KD mice had slightly less amounts of diet).

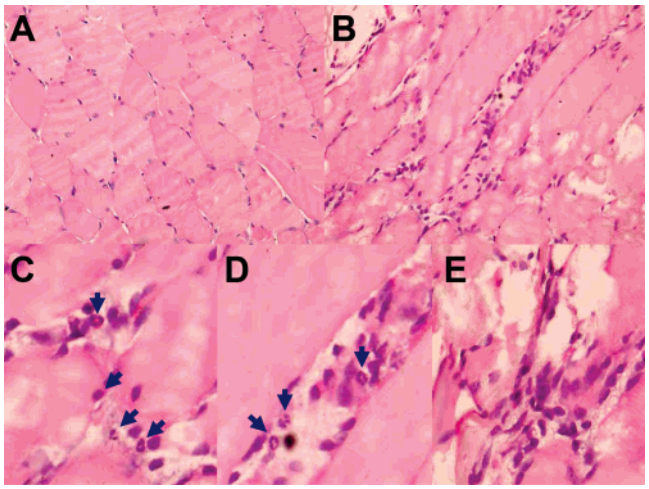

Figure 2. Histopathological findings. Sections of left gastrocnemius muscles were stained with hematoxylin-eosin. (A) Representative section of the normal murine muscles. (B) Representative section of the KD murine muscles that shows mild-degree infiltration of polymorphonuclear and mononuclear cells at some areas of the interstitium. The mentioned abnormal finding was found only in a few areas per section, whereas the remaining areas appeared normal. There was no vacuolization or inclusion body observed. (C−E) Polymorphonuclear (indicated with arrow heads) and mononuclear cells. Original magnification powers were 200× in (A) and (B) and 400× in (C−E).

of the interstitium of the KD muscles (Figure 2). The mentioned abnormal finding was found only in a few areas per section, whereas the remaining areas appeared normal. Neither vacuolization nor inclusion body was observed. The absence of vacuolization in our murine model of hypokalemic myopathy was not surprising as vacuolization was not found in all cases of human hypokalemic myopathy. In addition, degree and duration of potassium depletion might be the important factors for the characteristic vacuolization.

Altered Proteome in K^+-Depleted Muscles. The muscles were ground and resuspended in a lysis buffer (detailed in Materials and Methods section). Muscle proteins extracted from each animal were resolved in individual 2-D gel (n = 5 gels for 5 animals in each group) using board-range (pI 3−10, linear) IPG strips. The separated proteins were then visualized with

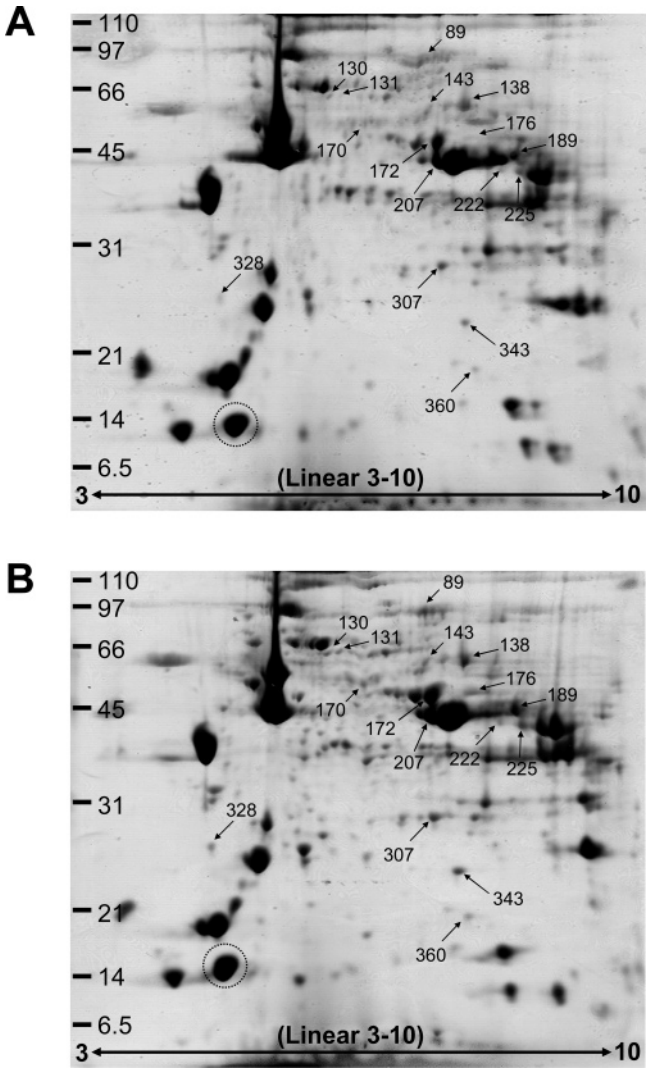

Figure 3. Proteome map of differentially expressed proteins between normal and KD mice. (A) Representative 2-D gel of the normal murine muscle proteome. (B) Representative 2-D image for muscle proteome of the KD mice. Equal amount of 200 μg total protein extracted from left gastrocnemius muscles was loaded in individual IPG strip and resolved by 2-DE ($n = 5$ gels from 5 different animals in each group). Separated proteins were then visualized by Coomassie Blue R-250 stain. Quantitative intensity analysis was performed and only significant differences between the two groups were subjected to identification, using MS peptide mass fingerprinting and MS/MS peptide sequencing, and are labeled. Numbers of protein spots correspond to those reported in Tables 1 and 2. The spot in the circled area and spot #307 were selected for further analysis of the variability (see Figure 5).

Coomassie Brilliant Blue R-250 stain. Using 2-D analysis software and highly stringent criteria for spot detection (described in details in Materials and Methods section), approximately 260 protein spots were visualized in each 2-D gel. Figure 3A illustrates a representative 2-D gel of the normal controls, whereas Figure 3B shows a representative 2-D gel of the KD muscles.

Quantitative intensity analysis revealed significantly differential expression of 16 protein spots between the two groups (Figure 3 and Table 1). Interestingly, the intensity levels of all differentially expressed spots were increased in the KD muscles. The degree of the up-regulation ranged from 1.21- to 8.27-fold. Using MALDI-MS, 13 of these altered proteins were successfully identified (Table 1). The identities of 13 proteins obtained from peptide mass fingerprinting were confirmed by Q-TOF MS/MS sequencing (Table 2). Q-TOF MS/MS analyses not only provided consistent results with those obtained from peptide mass fingerprinting but also identified 2 additional proteins that were not able to be identified by peptide mass fingerprinting (spots # 343 and 360). Sequences of the peptides identified by Q-TOF MS/MS are provided in Table 2.

To confirm our proteomic data, 2-D Western blot analysis of β-enolase was performed. Figure 4 clearly illustrates that expression levels of at least two forms of β-enolase were obviously increased in the KD muscles. This finding was consistent with the proteomic data, in which two forms of β-enolase were detected to be up-regulated in the KD muscles.

Brief Descriptions and Functional Significance of the Altered Muscle Proteins. Of the 15 spots representing 14 unique proteins that were identified by either MS peptide mass fingerprinting or MS/MS sequencing, most of them were muscle enzymes, except only for myosin-binding protein H (#131), translationally controlled tumor protein, translationally controlled 1 (#328), and alpha-B Crystallin (#343). Using the Pathway Tools (http://bioinformatics.ai.sri.com/ptools/),[23−25] more details of these enzymes including their descriptions and metabolic pathways could be obtained and are provided in Table 3. Because these metabolic pathways (totally 25 pathways) are crucial for cellular function and bioenergetics, the up-regulation of several enzymes involving in these multiple pathways during prolonged K^+ deprivation might be associated with the pathogenic mechanisms of hypokalemic myopathy. Further functional studies are required to address roles or functional significance of these altered muscle enzymes in hypokalemia-induced muscle injury.

On the other hand, the up-regulation of muscle enzymes may be the result of muscle damage, and elevated muscle enzymes can be used as the biomarkers. Creatine kinase (CK) reversibly catalyzes the transfer of phosphate between ATP and various phosphogens (e.g., creatine phosphate). CK isoenzymes also play a central role in energy transduction in tissues with large, fluctuating energy demands, such as skeletal muscle, heart, brain and spermatozoa.[26] In clinical practice, the increase in serum CK level in the absence of cardiac or brain infarction indicates significant muscle damage and is generally used as the diagnostic marker for rhabdomyolysis and/or muscle injury.[10] In the present study, we identified the increase in muscle isoform of CK in murine skeletal muscles. Additional findings were severe hypokalemia and metabolic alkalosis. These data therefore strengthen our model of hypokalemic myopathy.

Alpha-B Crystallin belongs to the small heat shock protein (HSP) family.[27] This protein was initially found in eye lens to serve the function for transparency and refractive index of the lens. However, its expression is not limited only to eye lens.[28] It is generally known that various HSPs are expressed in skeletal muscles, including small HSPs (i.e., ubiquitin, alpha-B Crystallin, HSP20, and HSP27), HSP60, HSP70, and HSP90. There is evidence suggesting that HSP expression in muscle fiber is type-specific.[29] Like other chaperones, alpha-B Crystallin prevents stress-induced protein denaturation and precipitation by binding to unfolded or denatured proteins, thereby suppressing irreversible protein aggregation and consecutive cell damage.[30] We therefore propose that the increase in muscle alpha-B

Table 1. Differentially Expressed Muscle Proteins in Normal vs K^+-depleted (KD) Mice

spot no.	protein	NCBI ID[a]	accession	MS MOWSE Score	MS Z Score	MS/MS Ion Score	%coverage (MS, MS/MS)	theoretical p*I* /MW (kDa)	estimated p*I*/MW (kDa)	intensity (Normal) (Mean ± SEM)	intensity (KD) (Mean ± SEM)	ratio (KD /Normal)	*P* values
89	muscle glycogen phosphorylase Mus musculus]	gi|15277968	AAH12961	54	2.43	126	15, 4	6.7/98	7.3/91	0.0376 ± 0.0198	0.2236 ± 0.0625	5.95	0.022
130	dihydrolipoamide S-acetyltransferase precursor [Mus musculus]	gi|16580128	AAL02400	72	2.43	39	29, 3	5.7/59	6.2/66	0.0054 ± 0.0054	0.0445 ± 0.0048	8.27	0.001
131	myosin-binding protein H (MyBP-H) (H-protein)	gi|6093458	P70402	124	2.43	105	44, 8	5.7/53	6.3/67	0.0054 ± 0.0035	0.0321 ± 0.0081	5.97	0.017
138	pyruvate kinase M [Mus musculus]	gi|551295	BAA07457	153	2.43	128	37, 13	7.6/58	7.8/63	0.2506 ± 0.0372	0.3606 ± 0.0329	1.44	0.049
143	dihydrolipoamide dehydrogenase [Mus musculus]	gi|2078522	AAC53170	65	2.43	80	23, 8	8.0/55	7.4/62	0.0406 ± 0.0175	0.0891 ± 0.0093	2.19	0.040
170	unidentified	NA[b]	NA[b]	NA[b]	NA[b]	NA[b]	NA, NA[b]	NA/NA[b]	6.6/53	0.0426 ± 0.0112	0.0848 ± 0.0142	1.99	0.048
172	enolase 3, beta muscle [Mus musculus]	gi|15488630	AAH13460	257	2.43	261	56, 12	6.7/47	7.4/49	0.8635 ± 0.0413	1.1278 ± 0.0595	1.31	0.006
176	enolase 3, beta muscle [Mus musculus]	gi|15488630	AAH13460	193	2.43	114	50, 6	6.7/47	7.9/50	0.0209 ± 0.0209	0.1392 ± 0.0169	6.65	0.002
189	phosphoglycerate kinase (EC 2.7.2.3) - mouse	gi|91176	A25567	76	2.43	142	29, 7	7.5/45	8.4/44	0.2036 ± 0.1260	0.6682 ± 0.0162	3.28	0.006
207	creatine kinase, muscle [Mus musculus]	gi|6671762	NP_031736	209	2.43	286	56, 20	6.6/43	7.4/43	0.8461 ± 0.0278	1.0394 ± 0.0536	1.23	0.013
222	NAD(P) dependent steroid dehydrogenase-like [Mus musculus]	gi|18043286	AAH19945	NA[b]	2.43	NA[b]	21, NA[b]	8.4/41	8.2/42	0.0292 ± 0.0185	0.0828 ± 0.0108	2.83	0.037
225	aldolase 1, A isoform [Mus musculus]	gi|42490830	AAH66218	88	2.43	149	36, 16	8.5/40	8.5/42	0.1010 ± 0.0441	0.2631 ± 0.0249	2.61	0.013
307	triosephosphate isomerase 1 [Mus musculus]	gi|6678413	NP_033441	158	2.43	346	53, 24	6.9/27	7.4/29	0.1678 ± 0.0101	0.2035 ± 0.0075	1.21	0.022
328	tumor protein, translationally controlled 1 [Mus musculus]	gi|6678437	NP_033455	51	2.43	261	25, 22	4.8/20	4.8/26	0.0223 ± 0.0092	0.0565 ± 0.0081	2.53	0.024
343	crystallin, alpha B [Mus musculus]	gi|6753530	NP_034094	NA[b]	NA[b]	55	NA, 9	6.8/20	7.7/24	0.0530 ± 0.0073	0.1005 ± 0.0180	1.90	0.040
360	nucleoside-diphosphate kinase 1 [Mus musculus]	gi|13542867	AAH05629	NA[b]	NA[b]	47	NA, 7	6.8/17	7.9/20	0.0576 ± 0.0062	0.0821 ± 0.0077	1.43	0.037

[a] NCBI = National Center for Biotechnology Information [b] NA = Not available

Table 2. Sequencing of Differentially Expressed Proteins Using Q-TOF MS/MS

spot no.	protein	ion scores	coverage (%)	identified peptides	residues
89	muscle glycogen phosphorylase [Mus musculus]	126	4	ARPEFTLPVHFYGR	193−206
				VLYPNDNFFEGKELR	279−293
				HLQIIYEINQR	400−410
130	dihydrolipoamide S-acetyltransferase precursor [Mus musculus]	39	3	VAPAPAGVFTDIPISNIR	324−341
131	myosin-binding protein H (MyBP-H) (H-protein)	105	8	NLALGDKFFLR	140−150
				ASIDILVIEKPGPPSSIK	268−280
				TGQWFTVLER	316−325
138	pyruvate kinase M [Mus musculus]	128	13	LNFSHGTHEYHAETIK	74−89
				EATESFASDPILYRPVAVALDTK	93−115
				FGVEQDVDMVFASFIR	231−246
				RFDEILEASDGIMVAR	279−294
143	dihydrolipoamide dehydrogenase [Mus musculus]	80	8	ALLNNSHYYHMAHGKDFASR	90−109
				IGKFPFAANSR	418−428
				VCHAHPTLSEAFR	483−495
172	enolase 3, beta muscle [Mus musculus]	261	12	IGAEVYHHLKGVIK	184−197
				TAIQAAGYPDKVVIGMDVAASEFYR	229−253
				IEEALGDKAVFAGR	413−426
176	enolase 3, beta muscle [Mus musculus]	114	6	IGAEVYHHLK	184−193
				IGAEVYHHLKGVIK	184−197
				IEEALGDKAVFAGR	413−426
189	phosphoglycerate kinase (EC 2.7.2.3) - mouse	142	7	LGDVYVNDAFGTAHR	157−171
				ALESPERPFLAILGGAK	200−216
207	creatine kinase, muscle [Mus musculus]	286	20	GYTLPPHCSR	139−148
				SFLVWVNEEDHLR	224−236
				AGHPFMWNEHLGYVLTCPSNLGTGLR	267−292
				HPKFEEILTR	305−314
				GTGGVDTAAVGAVFDISNADR	321−341
225	aldolase 1, A isoform [Mus musculus]	149	16	PHPYPALTPEQK	2−13
				ADDGRPFPQVIK	88−99
				IGEHTPSALAIMENANVLAR	154−173
				CPLLKPWALTFSYGR	290−304
307	triosephosphate isomerase 1 [Mus musculus]	346	24	DLGATWVVLGHSER	86−99
				RHVFGESDELIGQK	100−113
				HVFGESDELIGQK	101−113
				VSHALAEGLGVIACIGEK	114−131
				VVLAYEPVWAIGTGK	161−175
328	tumor protein, translationally-controlled 1 [Mus musculus]	261	22	DLISHDELFSDIYK	6−19
				DLISHDELFSDIYKIR	6−21
				IREIADGLCLEVEGK	20−34
				GKLEEQKPER	101−110
343	crystallin, alpha B [Mus musculus]	55	9	TIPITREEKPAVAAAPK	158−174
360	nucleoside-diphosphate kinase 1 [Mus musculus]	47	7	TFIAIKPDGVQR	7−18

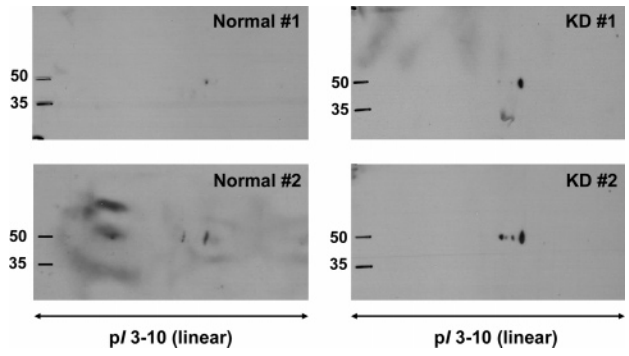

Figure 4. 2-D Western blot analysis of β-enolase. Muscle proteins resolved with 2-DE (totally 50 μg per gel) were transferred onto a nitrocellulose membrane and probed with rabbit polyclonal anti-β-enolase antibody (1:200 in 5% milk in PBS) and subsequently with swine anti-rabbit IgG conjugated with horseradish peroxidase (1:1000 in 5% milk in PBS). Reactive protein spots were then visualized with a chemiluminescence substrate. N = 2 individual animals in each group.

Crystallin in our model may be the regulatory mechanism for muscle injury and damage during hypokalemic stress.

Translationally controlled tumor protein (TCTP) belongs to the TCTP family that is involved in calcium binding and microtubule stabilization.[31,32] TCTP was originally identified as a serum-inducible 23-kDa protein that undergoes an early and prominent increase upon serum stimulation in cultured cells.[33] It was recently shown to be a tubulin-binding protein that interacts with microtubules during the cell cycle.[34] Recently, several reports highlighted the importance of TCTP for cell cycle progression and malignant transformation.[35] In addition, TCTP was shown to display an extracellular function as a histamine-releasing factor and to have anti-apoptotic activity.[36,37] These findings led to the other names or synonyms for this protein, including histamine-releasing factor (HRF)[36] and fortilin.[37] With a board range of cellular function, its role in hypokalemic myopathy, however, remains unknown and deserves further investigation.

Murine versus Rat Muscle Proteomes. In the present study, we identified a total of 15 protein spots representing 14 unique proteins that were regulated during chronic K^+ depletion in "BALB/c mice". Recently, Yan and colleagues[17] performed proteomic analysis and established initial 2-D reference maps of skeletal muscles from a "Wistar rat". Proteins derived from

Table 3. Brief Descriptions of Muscle Enzymes That Were Significantly Altered During Chronic Potassium Depletion

enzyme (*component of*)	synonyms	pathways
aldolase 1, A isoform (*EC reaction -lyases*)	fructose−1,6-bisphosphate aldolase	Calvin cycle
	fructose−1,6-bisphosphate triosephosphate-lyase	formaldehyde assimilation II (RuMP cycle)
	fructose-bisphosphate aldolase	fructose degradation to pyruvate and lactate (anaerobic)
		gluconeogenesis
		glycolysis I
		glycolysis II
		glycolysis IV
		mannitol degradation I
		sorbitol degradation
		sorbitol fermentation to lactate, formate, ethanol and acetate
		sucrose degradation to ethanol and lactate (anaerobic)
		xylulose-monophosphate cycle
creatine kinase, muscle (*EC reaction - transferases*)	none	interconversion of creatine and creatine phosphate
dihydrolipoamide S-acetyltransferase precursor (*Pyruvate dehydrogenase multienzyme complexes*)	E2	pyruvate degradation II
	lipoate acetyltransferase	
	pyruvate dehydrogenase complex E2 components	
	thioltransacetylase A	
dihydrolipoamide dehydrogenase (*EC reaction - oxidoreductases*)	diaphorase	interconversion of dihydrolipoamide and lipoamide
	dihydrolipoyl dehydrogenase	
	E3 component of alpha-ketoacid dehydrogenase complexes	
	lipoamide reductase	
	lipoyl dehydrogenase	
enolase 3, beta muscle (*degradosome*)	2,3-diphospho-D-glycerate, 2-phospho-D-glycerate phosphotransferase	gluconeogenesis
	2-phospho-D-glycerate hydrolyase	glycolysis I
	2-phosphoglycerate dehydratase	respiration (anaerobic)
	phosphopyruvate hydratase	
muscle glycogen phosphorylase (*glycogen phosphorylase/glycogen-maltotetraose phosphorylase*)	1,4-alpha-D-glucan:orthophosphate alpha-D-glucosyltransferase	glycogen degradation
	amylophosphorylase	
	polyglucose phosphorylase	
	polyphosphorylase	
nucleoside-diphosphate kinase 1 (*nucleoside diphosphate kinase/ UDP kinase/ CDP kinase/ dUDP kinase/ dCDP kinase/ dTDP kinase/ dADP kinase/ dGDP kinase*)	ATP-nucleoside diphosphate phosphotransferase	*de novo* biosynthesis of pyrimidine ribonucleotides
	NDK, NDP kinase	*de novo* biosynthesis of pyrimidine deoxyribonucleotides
	nucleoside 5′-diphosphate phosphotransferase	purine nucleotides *de novo* biosynthesis I
	nudiki	salvage pathway of pyrimidine nucleotides
phosphoglycerate kinase (EC 2.7.2.3) (*EC reaction - transferases*)	phosphoglycerate phosphorylase	2-dehydro-D-gluconate degradation
		Calvin cycle
		fructose degradation to pyruvate and lactate (anaerobic)
		gluconeogenesis
		glucose fermentation to lactate II
		glucose heterofermentation to lactate I
		glyceraldehyde−3-phosphate degradation
		glycolysis I
		glycolysis IV
		sorbitol fermentation to lactate, formate, ethanol and acetate
		sucrose degradation to ethanol and lactate (anaerobic)
pyruvate kinase M (*pyruvate kinase subunit*)	ATP:pyruvate 2-*O*-phosphotransferase	glycolysis I
	phosphoenol transphosphorylase	
	phosphoenolpyruvate kinase	
triosephosphate isomerase 1 (*EC reaction - isomerases*)	phosphotriose isomerase	Calvin cycle
	triose phosphate isomerase	fructose degradation to pyruvate and lactate (anaerobic)
	triose phosphoisomerase	glycolysis I
	triosephosphate mutase	glycolysis II
		glycolysis IV
		sorbitol fermentation to lactate, formate, ethanol and acetate
		sucrose degradation to ethanol and lactate (anaerobic)

"abdominal" skeletal muscles were resolved using two ranges of IPG strips, with p*I* 3−10 (nonlinear) and p*I* 4−7 (linear). A total of 652 and 697 protein spots, respectively, were detected by silver stain, and a total of 74 proteins were identified. Of these identified proteins, pyruvate kinase M, β-enolase, creatine kinase M, aldolase, triosephosphate isomerase 1, and alpha-B Crystallin were also identified in our murine model of hypokalemic myopathy. However, muscle glycogen phosphorylase, dihydrolipoamide S-acetyltransferase precursor, dihydrolipoamide dehydrogenase, myosin-binding protein H, phosphoglycerate kinase, NAD(P)-dependent steroid dehydrogenase-like protein, TCTP, and nucleoside-diphosphate kinase 1 that were identified from "gastrocnemius" muscles in our present study were not identified in their study. These differences might simply imply the differential expression of muscle proteins in different species of rodents. However, some technical issues should be taken into account for these differences. We analyzed "gastrocnemius" muscles, whereas they identified proteins from skeletal muscles at "abdominal wall". Moreover, both of these studies have not identified all of the visualized protein spots. We selectively identified only the regulated proteins affected by chronic K^+ depletion, whereas they selectively analyzed only 100 spots from >1000 spots visualized. Thus, a lot of proteins remain unidentified in both studies.

Serum Levels of Creatine Kinase (CK) and β-Enolase. To assess whether levels of some of the up-regulated muscle enzymes were also increased in the serum, we measured total CK (using Oliver-Rosalki assay[21,22]), CK−MM (using Western blot analysis), and CK−MB (using an ELISA) levels in sera of all 10 animals. The results indicated that serum total CK, CK−MM, and CK−MB levels were all negative (or under the detectable limits of their respective methods) in all the samples (both in normal and KD groups). Moreover, Western blot analysis of β-enolase, while provided a promising data on muscles as shown in Figure 4, showed the negative result in the sera of both normal and KD groups. Considering these data together with the histopathological findings, they might implicate that hypokalemic myopathy in our murine model was not as severe as rhabdomyolysis in humans. However, as we performed all the experiments and histopathological examination at the time-point of 8 weeks of K^+ depletion, serial analyses including the earlier and later time-points should be performed to address whether rhabdomyolysis has not occurred in our murine model or it might occur at the very early time-point but was finally recovered; thus, negative findings were obtained for serum markers.

Technical Concerns. (i) One of the most critical issues for gel-based, proteomic analysis is the reproducibility and comparability of 2-D spot pattern in different 2-D gels. To address this issue in our present study, we evaluated the coefficient of variation (CV) of a selected protein spot (circled in Figure 3) across 10 different gels. %CV was calculated by dividing the standard deviation by mean of intensity volume of the corresponding spot and multiplying by 100. Figure 5A shows the zoom-in, cropped images of the selected spot in all gels. Intragroup %CVs of this spot were 14.45% and 11.42% for the normal and KD mice, respectively. %CV of this spot for both groups was only 12.33% when the intensities of this spot in all 10 gels were considered. As this selected spot was quite intense and might be saturated, we also evaluated the CV of another spot (#307 in Figure 3) with much less intensity. Figure 5B shows the consistent results and demonstrates that intragroup %CVs of spot #307 were 13.50% and 8.19% for the normal and KD mice, respectively. %CV of this spot for both groups was only 14.30% when the intensities of this spot in all 10 gels were used for the calculation.

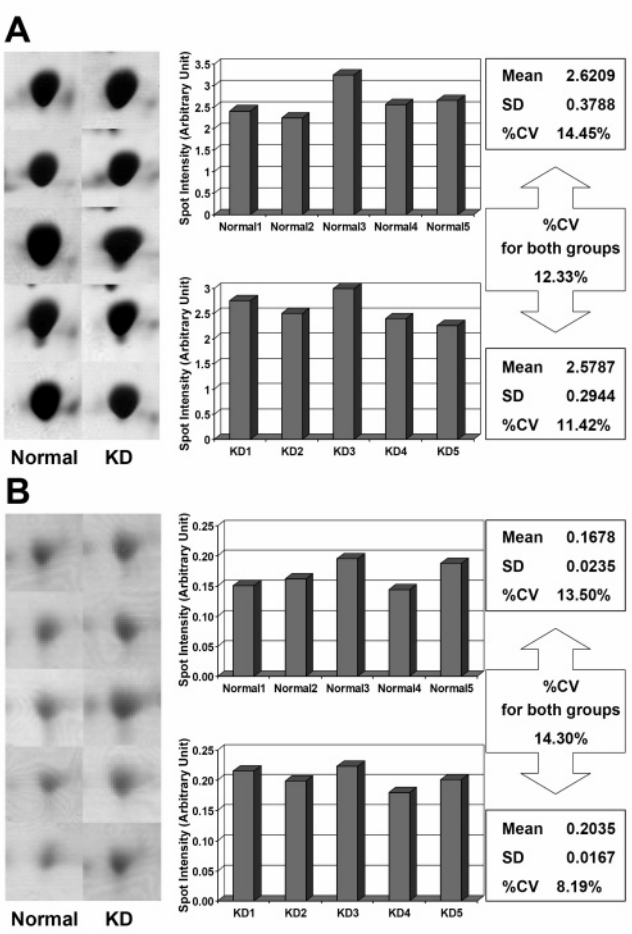

Figure 5. Variability. Zoom-in images of the selected spots from individual 2-D gels ($n = 5$ for each group). (A) Spot that is circled in Figure 3. (B) Spot #307. Coefficient of variation (CV) was then calculated (%CV = (standard deviation/mean) × 100%).

Considering all spots presented in each gel together, overall %CVs ($\%CV_{total}$) were 13.35, 11.37, and 11.84% for normal, KD, and both groups, respectively. In previous gel-based, proteome studies of human tissues, cell lines, and body fluids, up to 25% of CV was observed and acceptable for the reproducibility of 2-DE.[38−40] Hence, our results were justified for the standard quantitative differential proteomics. We also demonstrated that normalization of spot intensity in our present study was justified for the comparability of intensity volume of each protein spot across different gels, as the summation of normalized intensity volumes of all spots in each 2-D gel was comparable between groups (76.36 ± 4.56 and 79.42 ± 4.04 arbitrary units for normal and KD mice, respectively; p value was 0.629).

(ii) As discussed above, we have been very concerned for the inter-individual variability among different animals within or between groups. We performed the proteomic analysis using only one gel per animal and, thus, did not address an issue of intraindividual or interassay variability in the present study because several recent articles, by our[41] and other groups,[42] have readily demonstrated that the 2-D spot pattern is highly reproducible when the identical protocols and standardized parameters are used for different assays of the same sample.

However, to demonstrate that our present study was standardized and justified, we also performed 2-DE of a set of triplicates, which were resolved separately in different experiments. The data clearly confirmed that the 2-D spot pattern was essentially identical among the three gels that were run on different occasions (see Figure S1 in the Supporting Information).

(iii) The total number of protein spots visualized in the present study was relatively small for the muscle proteome. This could be explained by some technical limitations. First, we used a small format 2-D gel in the present study that has considerable limitations in protein separation; much more spots should have been resolved using a large format (using 18 to 24-cm-long IPG strip). Second, Coomassie Brillaiant Blue R-250 stain was employed in our present study. Much more spots would be expected to be detectable with the more sensitive stains; i.e., silver, fluorescence dyes, and colloidal Coomassie. Finally, we used the highly stringent criteria or parameters for detection of "true protein spots" (see Materials and Methods section). The total number of detected spots would be greater if the lower stringent criteria or parameters were used.

(iv) It should be noted that all the animals in the present study had metabolic alkalosis. Changes in blood pH might be one of the factors contributing to altered proteome in the KD muscles and should be taken into account for the interpretation of our data. Finally, we have not performed the experiment comparing changes due to hypokalemic myopathy to those caused by other forms of myopathy. It would be interesting to determine whether the findings in our present study are specific for hypokalemic myopathy and to evaluate whether these abnormal findings can be recovered after treatment with K^+ repletion.

Conclusions

We have demonstrated that prolonged K^+ depletion caused alterations in several muscle proteins in mice. Most of these altered proteins were enzymes that are involved in several various metabolic pathways and are crucial for cellular function and bioenergetics. These data may lead to a new roadmap for research on hypokalemic myopathy and to biomarker discovery. Our findings also underscore the potential use of proteomics to unravel the pathogenic mechanisms and pathophysiology of human diseases.

Abbreviations: ACN, acetonitrile; CHAPS, 3-[(3-cholamidopropyl)dimethylamino]-1-propanesulfonate; CHCA, α-cyano-4-hydroxycinnamic acid; CK, creatine kinase; CV, coefficient of variation; DTT, dithiothreitol; HRF, histamine-releasing factor; HSP, heat shock protein; KD, K^+-depleted; MALDI, matrix-assisted laser desorption/ionization; MOWSE, molecular weight search; MS, mass spectrometry; MS/MS, tandem mass spectrometry; Q-TOF, quadrupole time-of-flight; SDS, sodium dodecyl sulfate; TFA, trifluoroacetic acid; TCTP, translationally controlled tumor protein

Acknowledgment. We thank Somchai Chutipongtanate, Wipawanee Kasemworaphoom, Napat Songtawee, Theptida Semangoen, and Lt. Col. Duangporn Phulsuksombati for their technical assistance and Drs. Sumalee Nimmannit, Yasushi Nakagawa, Somkiat Vasuvattakul, Pa-thai Yenchitsomanus, and Suchai Sritippayawan for their advice. This study was supported by the Thailand Research Fund to P. Malasit (Senior Research Scholar Program; Grant #RTA4680017) and by Vejdusit Foundation to V.T.

Supporting Information Available: A set of triplicates of 2-D gels derived from the same muscle sample that were run separately in different experiments (Figure S1). The data show the essentially identical pattern of 2-D spots among different gels. This material is available free of charge via the Internet at http://pubs.acs.org.

References

(1) Cohn, J. N.; Kowey, P. R.; Whelton, P. K.; Prisant, L. M. New guidelines for potassium replacement in clinical practice: a contemporary review by the National Council on Potassium in Clinical Practice. *Arch. Intern. Med.* **2000**, *160*, 2429−2436.
(2) Mount, D. B.; Zandi-Nejad, K. Disorders of potassium balance. In *Brenner & Rector's The Kidney*, 7th ed.; Brenner, B. M., Ed.; W. B. Saunders: Philadelphia, 2004; pp 997−1040.
(3) Gennari, F. J. Hypokalemia. *N. Engl. J. Med.* **1998**, *339*, 451−458.
(4) Gennari, F. J. Disorders of potassium homeostasis. Hypokalemia and hyperkalemia. *Crit. Care Clin.* **2002**, *18*, 273−88., vi.
(5) Antes, L. M.; Kujubu, D. A.; Fernandez, P. C. Hypokalemia and the pathology of ion transport molecules. *Semin. Nephrol.* **1998**, *18*, 31−45.
(6) Tang, N. L.; Hui, J.; To, K. F.; Ng, H. K.; Hjelm, N. M.; Fok, T. F. Severe hypokalemic myopathy in Gitelman's syndrome. *Muscle Nerve* **1999**, *22*, 545−547.
(7) Satoh, J.; Kuroda, Y.; Nawata, H.; Yanase, T. Molecular basis of hypokalemic myopathy caused by 17alpha-hydroxylase/17,20-lyase deficiency. *Neurology* **1998**, *51*, 1748−1751.
(8) Finsterer, J.; Hess, B.; Jarius, C.; Stollberger, C.; Budka, H.; Mamoli, B. Malnutrition-induced hypokalemic myopathy in chronic alcoholism. *J. Toxicol. Clin. Toxicol.* **1998**, *36*, 369−373.
(9) Allison, R. C.; Bedsole, D. L. The other medical causes of rhabdomyolysis. *Am. J. Med. Sci.* **2003**, *326*, 79−88.
(10) Warren, J. D.; Blumbergs, P. C.; Thompson, P. D. Rhabdomyolysis: a review. *Muscle Nerve* **2002**, *25*, 332−347.
(11) Ng, Y. C. Hypokalemia downregulates cardiac alpha 1 and skeletal muscle alpha 2 isoforms of Na+,K(+)-ATPase in ferrets. *Biochem. Biophys. Res. Commun.* **1993**, *196*, 39−46.
(12) McDonough, A. A.; Thompson, C. B. Role of skeletal muscle sodium pumps in the adaptation to potassium deprivation. *Acta Physiol. Scand.* **1996**, *156*, 295−304.
(13) Thompson, C. B.; Choi, C.; Youn, J. H.; McDonough, A. A. Temporal responses of oxidative vs. glycolytic skeletal muscles to K+ deprivation: Na+ pumps and cell cations. *Am. J. Physiol.* **1999**, *276*, C1411−C1419.
(14) Thongboonkerd, V. Proteomic analysis of renal diseases: Unraveling the pathophysiology and biomarker discovery. *Expert Rev. Proteomics* **2005**, *2*, 349−366.
(15) Marko-Varga, G.; Fehniger, T. E. Proteomics and disease−the challenges for technology and discovery. *J. Proteome Res.* **2004**, *3*, 167−178.
(16) Petricoin, E.; Wulfkuhle, J.; Espina, V.; Liotta, L. A. Clinical proteomics: revolutionizing disease detection and patient tailoring therapy. *J. Proteome Res.* **2004**, *3*, 209−217.
(17) Yan, J. X.; Harry, R. A.; Wait, R.; Welson, S. Y.; Emery, P. W.; Preedy, V. R.; Dunn, M. J. Separation and identification of rat skeletal muscle proteins using two-dimensional gel electrophoresis and mass spectrometry. *Proteomics* **2001**, *1*, 424−434.
(18) van den Heuvel, L. P.; Farhoud, M. H.; Wevers, R. A.; van Engelen, B. G.; Smeitink, J. A. Proteomics and neuromuscular diseases: theoretical concept and first results. *Ann. Clin. Biochem.* **2003**, *40*, 9−15.
(19) Shishkin, S. S.; Kovalyov, L. I.; Kovalyova, M. A. Proteomic studies of human and other vertebrate muscle proteins. *Biochemistry (Mosc.)* **2004**, *69*, 1283−1298.
(20) Cagney, G.; Park, S.; Chung, C.; Tong, B.; O'Dushlaine, C.; Shields, D. C.; Emili, A. Human tissue profiling with multidimensional protein identification technology. *J. Proteome Res.* **2005**, *4*, 1757−1767.
(21) Miyada, D. S.; Dinovo, E. C.; Nakamura, R. M. Creatine kinase reactivation by thiol compounds. *Clin. Chim. Acta* **1975**, *58*, 97−99.
(22) Nealon, D. A.; Henderson, A. R. The apparent Arrhenius relationships of the human creatine kinase isoenzymes using the Oliver-Rosalki assay. *Clin. Chim. Acta* **1976**, *66*, 131−136.
(23) Karp, P. D.; Paley, S.; Romero, P. The Pathway Tools software. *Bioinformatics* **2002**, *18* (Suppl 1), S225−S232.
(24) Karp, P. D.; Krummenacker, M.; Paley, S.; Wagg, J. Integrated pathway-genome databases and their role in drug discovery. *Trends Biotechnol.* **1999**, *17*, 275−281.

(25) Karp, P. D.; Paley, S. Integrated access to metabolic and genomic data. *J. Comput. Biol.* **1996**, *3*, 191−212.
(26) Trask, R. V.; Strauss, A. W.; Billadello, J. J. Developmental regulation and tissue-specific expression of the human muscle creatine kinase gene. *J. Biol. Chem.* **1988**, *263*, 17142−17149.
(27) Frederikse, P. H.; Dubin, R. A.; Haynes, J. I.; Piatigorsky, J. Structure and alternate tissue-preferred transcription initiation of the mouse alpha B-crystallin/small heat shock protein gene. *Nucleic Acids Res.* **1994**, *22*, 5686−5694.
(28) Dubin, R. A.; Wawrousek, E. F.; Piatigorsky, J. Expression of the murine alpha B-crystallin gene is not restricted to the lens. *Mol. Cell Biol.* **1989**, *9*, 1083−1091.
(29) Liu, Y.; Steinacker, J. M. Changes in skeletal muscle heat shock proteins: pathological significance. *Front Biosci.* **2001**, *6*, D12−D25.
(30) Ganea, E. Chaperone-like activity of alpha-crystallin and other small heat shock proteins. *Curr. Protein Pept. Sci.* **2001**, *2*, 205−225.
(31) Gross, B.; Gaestel, M.; Bohm, H.; Bielka, H. cDNA sequence coding for a translationally controlled human tumor protein. *Nucleic Acids Res.* **1989**, *17*, 8367.
(32) Yarm, F. R. Plk phosphorylation regulates the microtubule-stabilizing protein TCTP. *Mol. Cell Biol.* **2002**, *22*, 6209−6221.
(33) Benndorf, R.; Nurnberg, P.; Bielka, H. Growth phase-dependent proteins of the Ehrlich ascites tumor analyzed by one- and two-dimensional electrophoresis. *Exp. Cell Res.* **1988**, *174*, 130−138.
(34) Gachet, Y.; Tournier, S.; Lee, M.; Lazaris-Karatzas, A.; Poulton, T.; Bommer, U. A. The growth-related, translationally controlled protein P23 has properties of a tubulin binding protein and associates transiently with microtubules during the cell cycle. *J. Cell Sci.* **1999**, *112* (Pt 8), 1257−1271.
(35) Bommer, U. A.; Thiele, B. J. The translationally controlled tumour protein (TCTP). *Int. J. Biochem. Cell Biol.* **2004**, *36*, 379−385.
(36) MacDonald, S. M.; Rafnar, T.; Langdon, J.; Lichtenstein, L. M. Molecular identification of an IgE-dependent histamine-releasing factor. *Science* **1995**, *269*, 688−690.
(37) Li, F.; Zhang, D.; Fujise, K. Characterization of fortilin, a novel antiapoptotic protein. *J. Biol. Chem.* **2001**, *276*, 47542−47549.
(38) Hunt, S. M.; Thomas, M. R.; Sebastian, L. T.; Pedersen, S. K.; Harcourt, R. L.; Sloane, A. J.; Wilkins, M. R. Optimal replication and the importance of experimental design for gel-based quantitative proteomics. *J. Proteome Res.* **2005**, *4*, 809−819.
(39) Terry, D. E.; Desiderio, D. M. Between-gel reproducibility of the human cerebrospinal fluid proteome. *Proteomics* **2003**, *3*, 1962−1979.
(40) Molloy, M. P.; Brzezinski, E. E.; Hang, J.; McDowell, M. T.; VanBogelen, R. A. Overcoming technical variation and biological variation in quantitative proteomics. *Proteomics* **2003**, *3*, 1912−1919.
(41) Klein, E.; Klein, J. B.; Thongboonkerd, V. Two-dimensional gel electrophoresis: a fundamental tool for expression proteomics studies. *Contrib. Nephrol.* **2004**, *141*, 25−39.
(42) Witzmann, F. A.; Li, J. Cutting-edge technology. II. Proteomics: core technologies and applications in physiology. *Am. J. Physiol. Gastrointest. Liver Physiol.* **2002**, *282*, G735−G741.

PR060136H